Supporting Information

The Effect of Humidity on the Interaction of Dimethyl Methylphosphonate (DMMP) Vapor with SiO_2 and Al_2O_3 Surfaces, Studied Using Infrared Attenuated Total Reflection Spectroscopy[*]

V.M. Bermudez

Naval Research Laboratory

Washington, DC 20375-5347

S1. Procedure for determining SiO_2 thickness using XPS

Figures S1 and S2 show typical XPS data for SiO_2 films prepared as described in the main text. The Si 2p data (Fig. S2a) show a peak from the substrate, which is partially resolved into a $2p_{1/2}$ and $2p_{3/2}$ spin-orbit doublet, and a peak from SiO_2, which is too broad to resolve. Other features, due to SiO_x ($x<2$) at the interface[1], are not readily observable. The relative integrated area, after background subtraction, is given by[2]

$$\frac{I_{ox}}{I_{Si}} = \frac{N_{ox}\sigma_{ox}V_s^{ox}}{N_{Si}\sigma_{Si}V_s^{Si}e^{-d_{ox}/\lambda_{ox}\cos\varphi}} \qquad \text{(S1)}$$

where I is the integrated area of the SiO_2 or the Si peak, N is the number of Si atoms per unit volume in either material, σ is the Si 2p photoionization cross-section, and V_s is the volume sampled. In the situation of interest here, all the other terms influencing the XPS intensity[2] (detector gain, analyzer transmission, etc.) cancel in the ratio. The exponential term in the denominator accounts for the attenuation of the substrate peak by the oxide layer of thickness d_{ox}. λ_{ox} is the elec-

[*] All references cited in the Supporting Information are listed at the end of this section and not in the main text.

Report Documentation Page

Form Approved
OMB No. 0704-0188

1. REPORT DATE	2. REPORT TYPE	3. DATES COVERED
2010		**00-00-2010 to 00-00-2010**

4. TITLE AND SUBTITLE	5a. CONTRACT NUMBER
Supporting Information for The Effect of Humidity on the Interaction of Dimethyl Methylphosphonate (DMMP) Vapor with SiO2 and Al2O3 Surfaces, Studied Using Infrared Attenuated Total Reflection Spectroscopy	5b. GRANT NUMBER
	5c. PROGRAM ELEMENT NUMBER
6. AUTHOR(S)	5d. PROJECT NUMBER
	5e. TASK NUMBER
	5f. WORK UNIT NUMBER
7. PERFORMING ORGANIZATION NAME(S) AND ADDRESS(ES) **Naval Research Laboratory,Washington,DC,20375**	8. PERFORMING ORGANIZATION REPORT NUMBER
9. SPONSORING/MONITORING AGENCY NAME(S) AND ADDRESS(ES)	10. SPONSOR/MONITOR'S ACRONYM(S)
	11. SPONSOR/MONITOR'S REPORT NUMBER(S)

12. DISTRIBUTION/AVAILABILITY STATEMENT
Approved for public release; distribution unlimited

13. SUPPLEMENTARY NOTES

14. ABSTRACT

15. SUBJECT TERMS

16. SECURITY CLASSIFICATION OF:			17. LIMITATION OF ABSTRACT	18. NUMBER OF PAGES	19a. NAME OF RESPONSIBLE PERSON
a. REPORT	b. ABSTRACT	c. THIS PAGE			
unclassified	**unclassified**	**unclassified**	**Same as Report (SAR)**	**26**	

tron attenuation length (EAL) in the oxide (see below), and φ is the angle between the surface normal and the path of the detected electrons. N can be written as $N = n(\rho/M)N_A$ where n is the number of atoms of a given type per "molecule" (e.g, $n = 1$ for Si in SiO_2), ρ is the density of the material, M is the atomic or molecular weight and N_A is Avogadro's number. V_s can be written as $V_s = A_s d_s$ where A_s, the area sampled, is the same for either peak and cancels in the ratio. The sampling depth, d_s, is given by

$$d_s = \int_0^d e^{-x/\lambda\cos\varphi} dx = (\lambda\cos\varphi)(1 - e^{-d/\lambda\cos\varphi}) \qquad \text{(S2)}$$

where d is the thickness of the material. The integrand in Eq. (S2) gives the contribution to the total signal from a layer of thickness dx at a depth x below the surface. For the Si substrate, $d >> \lambda$, and d_s is then simply $\lambda_{Si}\cos\varphi$ in terms of the EAL in Si. Combining all these quantities gives

$$\frac{I_{ox}}{I_{Si}} = \frac{\rho_{ox} M_{Si} \sigma_{ox} \lambda_{ox}}{\rho_{Si} M_{ox} \sigma_{Si} \lambda_{Si}} (e^{+d_{ox}/\lambda_{ox}\cos\varphi} - 1) \qquad \text{(S3)}$$

If electrons traveled in straight lines through a solid then λ would simply be the inelastic mean free path. However, if elastic scattering is taken into account then determining the correct EAL becomes a complex problem in electron transport[3]. A database is available[4] that allows the EAL to be found using an analytical transport model that closely approximates the results of Monte Carlo calculations and that involves only a few simple material parameters (see below). Several definitions of the EAL are given[3-5], which depend on the physical problem to be analyzed. For the bulk Si substrate the desired quantity (λ_{Si}) is termed the "practical EAL for quantitative analysis" and is defined such that the correct sampling depth, including elastic scattering ef-

fects, is given by $\lambda_{Si}cos\varphi$. For the oxide, λ_{ox} is the "average practical EAL" for a film thickness reasonably close to the final value of d_{ox}.

The input parameters used in the database include φ (defined above) and γ, the angle between the x-ray beam and photoelectron path. For the XPS system used here (Thermo Scientific K-Alpha), $\varphi = 0$ and $\gamma = 54.7°$. The asymmetry parameter (β), describing the angular dependence of the photoelectron distribution for each core level, is also needed. These are given in ref 6. For an element (e.g., Si) the material parameters are contained within the database. For SiO_2 the additional quantities needed are ρ (given below), the band gap (E_g = 8.9 eV, ref 7) and the number of valence electrons per "molecule", N_v = 16 (4 for Si plus 6 for each O). The results for Al Kα excitation are λ_{ox} = 35.72 (35.43) Å for the UV/O_3 (thermal) oxide and λ_{Si} = 31.77 Å. For a very thin film the "average practical EAL" depends somewhat on thickness, and the slightly different EALs for the two types of SiO_2 are due to the different densities and thicknesses (2 nm for the UV/O_3 oxide and 8 nm for the thermal oxide, as given below). The other quantities need to evaluate Eq. (S3) are:

ρ (gm/cm^3) = 2.27 (UV/O_3 SiO_2; ref 8); 2.24 (thermal SiO_2; ref 8); 2.33 (Si; ref 9)

M (gm) = 60.08 (SiO_2); 28.08 (Si)

σ_{ox}/σ_{Si} = 1.1 (for Al Kα excitation, ref 1).

$\rho(SiO_2)$ for the UV/O_3 oxide was obtained[8] using grazing-incidence x-ray reflectometry for a film grown under conditions similar to those used here (λ_{UV} = 222 nm at 390 °C). The various quantities used in the surface analyses reported here are summarized in Table S1.

The final result for SiO_2 thickness is $d_{ox}(nm) = (3.57)ln[2.02(I_{ox}/I_{Si}) + 1]$ for the UV/O_3 oxide and $(3.54)ln[(2.06(I_{ox}/I_{Si})+1]$ for the thermal oxide. The relative peak area was determined by least-squares fitting (not shown) using a pair of Gaussian-broadened Lorentzian (Voigt) func-

tions for the Si spin-orbit doublet and a single Gaussian for the SiO_2 peak. The Lorentzian linewidth was fixed at 35 meV as determined[10] for bulk Si. These lineshape functions were added to a polynomial background function, and all lineshape and background parameters were unconstrained in the fitting process.

S2. Procedure for determining *a*-Al_2O_3 thickness using XPS

Figures S3 and S4 show data for Al_2O_3. The thickness was determined from the ratio of Al 2p and Si 2p peak intensities, I_{Al}/I_{Si}, using an expression similar to Eq. (S1)

$$\frac{I_{Al}}{I_{Si}} = \frac{N_{Al}\sigma_{Al}V_s^{Al}}{N_{Si}\sigma_{Si}V_s^{Si}e^{-d_{Al}/\lambda_{Al}\cos\varphi}} \qquad \text{(S4)}$$

where "Al" refers to Al_2O_3 and "Si" to elemental Si. In general, this should be multiplied by $[D(E_{Al})T(E_{Al})L_{Al\,2p}(\gamma,E_{Al})]/[D(E_{Si})T(E_{Si})L_{Si\,2p}(\gamma,E_{Si})]$ where $D(E_x)$ is the detector gain and $T(E_x)$ the analyzer transmission at the photoelectron kinetic energy E_x. In the Thermo Scientific K-Alpha system these terms are removed from the experimental intensities through calibration. The asymmetry factor[6] L (not to be confused with the asymmetry parameter β) is in all cases unity for $\gamma = 54.7°$. Following the procedure described above, Eq. (S4) reduces to

$$\frac{I_{Al}}{I_{Si}} = \frac{n_{Al}\rho_{Al}M_{Si}\sigma_{Al}\lambda'_{Al}(1-e^{-d_{Al}/\lambda'_{Al}\cos\varphi})}{n_{Si}\rho_{Si}M_{Al}\sigma_{Si}\lambda_{Si}e^{-d_{Al}/\lambda_{Al}\cos\varphi}} \qquad \text{(S5)}$$

where λ_{Al} (λ'_{Al}) is the average practical EAL for Si 2p (Al 2p) photoelectrons in the thin Al_2O_3 layer. As before, λ_{Si} is the EAL for Si 2p photoelectrons in bulk Si. The other terms have been described above, where the subscript Al now refers to Al_2O_3. To a good approximation $\lambda_{Al} \approx \lambda'_{Al}$ for Al Kα excitation (cf. Table S1), and Eq. (S5) reduces to

$$\frac{I_{Al}}{I_{Si}} = \frac{2\rho_{Al}M_{Si}\sigma_{Al}\lambda'_{Al}}{\rho_{Si}M_{Al}\sigma_{Si}\lambda_{Si}}\left(e^{+d_{Al}/\lambda'_{Al}} - 1\right) \qquad \text{(S6)}$$

If there is an SiO_2 layer of thickness d_{ox} at the Al_2O_3/Si interface then the attenuation of the Si 2p photoelectrons from the elemental Si substrate must be taken into account by including a factor of $exp(-d_{ox}/\lambda_{ox})$ in the denominator of Eq. S(6), where λ_{ox} is defined in Sec. S1. d_{ox} is easily obtained from the SiO_2/Si 2p intensity ratio, as in Sec. S1, since both peaks are attenuated to the same extent by the Al_2O_3 overlayer.

For the density of amorphous Al_2O_3 we used ρ_{Al} = 3.20 gm/cm^3 (ref 11), and σ_{Al}/σ_{Si} = 0.657 is given in ref 12. Since the total intensity for both 2p spin-orbit components is used for either element, the σ used in the ratio is the sum of the $2p_{1/2}$ and $2p_{3/2}$ contributions. For the computation of λ'_{Al}, the EAL for Al Kα-excited Al 2p and Si 2p photoelectrons in a thin layer of a-Al_2O_3, we used E_g = 5.1 eV for the band gap of a-Al_2O_3 (ref. 13). All other quantities have been given above. The result, λ'_{Al} = 28.51 Å for an 8 nm-thick film, shows little (<10%) dependence on reasonable variations in either ρ_{Al} or E_g. The final result for the a-Al_2O_3 thickness is then $d_{Al}\ (nm) = (2.85)ln[2.16(I_{Al}/I_{Si})+1]$ in the absence of interfacial Si oxide.

The above analysis was repeated for an hydroxylated film (Figs. S3 and S5), modeled as Al oxyhydroxide (AlO(OH)). The reason for this choice will be given in Sec. S7. In this case a density of ρ_{Al} = 3.03 gm/cm^3 was used, based on results[14] for the mineral boehmite. A band gap of ~5.6 eV is estimated from photoluminescence excitation data[15], which show an onset of the interband transition in boehmite powder at roughly 220 nm (5.6 eV). This leads to an EAL of λ'_{Al} = 30.41 Å for Si 2p and Al 2p photoelectrons in a 5 nm-thick film. With n_{Al} = 1 in Eq. S5 the final result is then $d_{Al}\ (nm) = 3.04ln[2.61(I_{Al}/I_{Si})+1]$ for the AlO(OH) thickness in the absence of an interfacial Si oxide.

S3. Procedure for determining surface contamination levels using XPS

For a submonolayer coverage of an atomic impurity species X, the XPS intensity of a core level relative to that of the O 1s is given by

$$\frac{I_x}{I_{ox}} = \frac{N_x \sigma_x}{\frac{n_{ox}\rho_{ox}N_A}{M_{ox}}\sigma_{ox}\lambda_{ox}\cos\varphi(1-e^{-d_{ox}/\lambda_{ox}\cos\varphi})} \qquad \text{(S6)}$$

where N_x is now the number of X atoms *per unit area* and n_{ox} = 2 for SiO_2. The other terms have been defined previously. The impurity coverage is assumed to be sufficiently small that attenuation of the substrate signal can be neglected. λ_{ox} is now redefined as the "average practical EAL" for Al Kα-excited O 1s photoelectrons in a thin film of SiO_2 or Al_2O_3. For a 2 nm-thick UV/O_3 oxide on Si, λ_{ox} = 26.01 Å is found using the procedure described above. d_{ox} is the oxide thickness determined above, and the denominator is simply the number of O atoms per unit volume in the oxide times the O 1s photoionization cross-section times the sampling depth. As described above, I_x/I_{ox} is assumed to have been corrected for the effects of analyzer transmission and detector sensitivity through appropriate calibration procedures, and the asymmetry factor is assumed to be unity (γ = 54.7°). The only additional quantities needed are σ_C/σ_O = 0.341 and σ_F/σ_O = 1.51 for the C_{1s}/O_{1s} and F_{1s}/O_{1s} ratios of Al Kα photoionization cross-sections[10]. For SiO_2 the results are $N_C = 1.69x10^{16}(I_C/I_{ox})$ and $N_F = 3.82x10^{15}(I_F/I_{ox})$ respectively for the C and F coverages in atoms/cm^2.

N_x can be expressed as a fraction of a monolayer ($\theta_x = N_x/N_O$) if N_O, the areal density of O atoms on the oxide surface, can be estimated. This is somewhat difficult for an amorphous material. Tielens et al.[16] have constructed a slab model of *a*-SiO_2 with a density of ρ = 1.7 gm/cm^3

and 8 Si/nm^2 on the surface. Scaling the Si areal density by $(2.27/1.7)^{2/3}$ to correct for the smaller ρ of the model *vs.* the real system, and assuming 2 surface O atoms for every surface Si, gives $N_O \approx 1.9\text{x}10^{15}$ atoms/cm^2 from which are obtained the final results $\theta_C \approx 8.9(I_C/I_O)$ and $\theta_F \approx 2.0(I_F/I_O)$ for the 2.1 nm-thick UV/O_3 oxide. A similar analysis for the 8.1 nm-thick thermal oxide, for which I_O is larger, gives $\theta_C \approx 15.1(I_C/I_O)$.

A similar procedure was applied for *a*-Al_2O_3 and for hydroxylated *a*-Al_2O_3, modeled as AlO(OH) (see Sec. S7 below). The only additional parameters needed are λ_{ox} = 20.28 and 21.68 Å respectively for the EAL of Al Kα-excited O 1s photoelectrons in an 8 nm-thick film of *a*-Al_2O_3 and a 5 nm-thick film of AlO(OH). With n_{ox} = 3 for Al_2O_3 and 2 for AlO(OH) and with appropriate values for d_{ox}, Eq. (S6) yields C coverages (atoms/cm^2) of $5.55\text{x}10^{16}(I_C/I_O)$ for the former and $3.57\text{x}10^{16}(I_C/I_O)$ for the later

S4. Procedure for determining oxide-layer stoichiometry using XPS

From the discussion given above one easily obtains an expression for the oxide stoichiometry n_O/n_M, where "O" refers to oxygen and "M" to the metal (Si or Al), given by

$$\frac{I_O}{I_M} = \frac{n_O \sigma_O \lambda_O (1 - e^{-d_{ox}/\lambda_O \cos\varphi})}{n_M \sigma_M \lambda_M (1 - e^{-d_{ox}/\lambda_M \cos\varphi})} \qquad \text{(S7)}$$

Here I_O is the O 1s peak area and I_M is the area of the oxidized Si or Al 2p doublet. λ_O and λ_M, the EAL's in the thin oxide layer, are given above. The oxide layer thickness, d_{ox}, is determined as described in Secs. S1 and S2 above. The only additional quantities needed are, from ref. 10, σ_O/σ_{Si} = 3.59 and σ_O/σ_{Al} = 5.46, where σ_M is the sum of the $2p_{1/2}$ and $2p_{3/2}$ terms.

S5. Surface analysis of *a*-SiO_2 using XPS

This section applies the formalism developed above to an analysis of the SiO_2 surfaces. Figure S1 shows XPS survey spectra for typical samples used in this work. The data show C and a small concentration of F as the only impurities. The carbon is an unavoidable consequence of exposure to ambient air and results from contamination by organic species. However, the small H_2O contact angles for these samples (always <10° and often <5°) show that the contaminant does not interfere with wetting of the surface. The F impurity is incurred during the UV/O_3 exposure as a result of O_3 attacking the Teflon clamp holding the UV lamp. The final treatment before mounting the sample in the ATR cell consists of immersion in RCA-1 solution followed by rinsing in H_2O. This is expected to replace any surface F with OH; hence, the small amount of F detected in XPS is thought to reside in the bulk of the oxide film rather than on the surface.

Figure S2 shows Si 2p, O 1s and C 1s data for UV/O_3 SiO_2. The binding energies (BEs) have been corrected slightly to bring the bulk Si $2p_{3/2}$ peak into agreement with the reference value[17] of 99.34 eV. This was necessitated by a small XPS charging shift (0.50 eV) resulting from the high resistivity of the Si ATR substrates. The region between the Si and SiO_2 Si 2p peaks shows little or no evidence of distinct features[1,8] due to sub-oxides (SiO_x, x<2). Such species must exist at the transition between Si and SiO_2, but they are apparently confined to the immediate interface in the present samples. The absence of prominent sub-oxide structure in the Si 2p spectrum indicates a stoichiometric oxide. The corrected BE of the O 1s peak, 532.8 eV, is in good agreement with literature results[18], which give 532.9±0.4 eV for SiO_2 based on an average of 36 independent values. A BE of 533.5 eV has been found[19] for an OH group on the SiO_2 surface; however, attempts to resolve an OH feature using least-squares fitting with a sum of Gaussians were unsuccessful.

The C 1s peak shows features at higher BE (i.e., a shoulder at ~287 eV and a weak peak at ~290 eV), which can be assigned to O-containing functional groups[19,20], most likely C-OH and/or C-O-C for the former and C=O for the latter. The BE of the main peak, about 285.5 eV, is higher than that of elemental (graphitic) carbon (284.44 eV, ref 17) but closer to values reported[20] for *n*-alkyl species. Thus it appears that most of the C contamination arises from aliphatic hydrocarbons, which would be weakly bonded to the SiO_2 surface and, therefore, easily displaced by H_2O or DMMP. The C coverage is ~$2.3x10^{15}$ atoms/cm^2, or 1.2 monolayers (MLs), which is an average of results for several different nominally-identical samples and sample areas. However, the *molecular* coverage will be substantially less. Thus if the average contaminant is an alkyl species with, say, 6 C atoms per molecule, the coverage of adsorbed molecules would be ~0.20 ML. A particular point of interest (see Sec. 3.1.2 in the main text) is the coverage of C=O species. From the area of the 290 eV peak relative to that of the O 1s a C=O coverage of ~0.08 ML is estimated. Similarly the average F coverage for the UV/O_3 oxide is estimated to be ~0.18 ML *assuming that the F is all on the surface.* However, as noted above, the F impurity is believed to be bound within the SiO_2 and not on the actual surface.

Finally, the atom ratio for the UV/O_3 (thermal) SiO_2 is found to be n_O/n_{Si} = 1.97 (1.90). Since the oxide is already known to be essentially stoichiometric, on the basis of the above discussion, n_O/n_{Si} is useful as a self-consistency check on the analytical procedure. The results obtained here are smaller, by 5% or less, than the ideal value of 2.0. This might be due in part to a small contribution from suboxides, SiO_x ($x<2$), at the SiO_2/Si interface. The results for thermal oxides are similar to those of the UV/O_3 samples except that the C coverage (not shown) was lower, ~0.78 ML, and no F 1s peak was detected.

The level of impurity C seen on these surfaces was a source of concern. However, three points should be noted in this regard. Firstly, samples with very different total C coverages showed no difference in any of the results reported. Secondly, the C coverage was not sufficiently high that it interfered with either the formation of the ice-like H_2O layer or the strong adsorption of DMMP at low P/P_0. A third point to note is that the samples used here were in a sealed environment (i.e., the ATR flow cell) under continuous dry-N_2 purge, except when exposed to either H_2O or DMMP. This combination of environments is expected to remove all but strongly-adsorbed organic species. Hence, the C coverage detected under vacuum in XPS is thought to be a fair representation of the impurity level on the actual experimental surfaces. In other words, the C coverages on the IR ATR samples will not be higher than those observed in XPS.

S6. Surface analysis of Al_2O_3 using XPS

This section presents an analysis of the *a*-Al_2O_3 XPS data (Figs. S3 and S4). The Al, C and O BEs were shifted so as to bring the main C 1s peak to 285.5 eV in agreement with the SiO_2 data discussed in Sec. S5. The required BE correction of -1.4 eV is consistent with a positive charge on the oxide layer. However, the Si $2p_{3/2}$ peak appeared at 99.3 eV in the raw data, which is essentially identical to the reference value[17]. The Si 2p spectrum is weak, due to attenuation by the Al_2O_3 overlayer, and the peak position was obtained accurately by least-squares fitting (not shown) with a sum of Gaussian functions and a polynomial background. The absence of a significant Si 2p shift indicates that the oxide BE shift is due to a variation in the position of the Fermi level in the oxide band gap rather than to an actual charging of the sample. This phenomenon has been discussed previously[21,22] in connection with XPS data for Al_2O_3 films. In this situation, using the C 1s for BE referencing provides only an approximate correction.

The Al 2p peak, at 74.5 eV, can be fitted with a single Voigt-function spin-orbit doublet (not shown) and gives no indication of any sub-oxide features at lower BE. In metallic Al, for example, the 2p BE is about 73 eV (ref 17). The Si 2p data show about 6.5 nm of SiO_2 at the Al_2O_3/Si interface. The O 1s peak is noticeably more broad and asymmetric than in the case of SiO_2 (Fig. S2). It is similar in appearance to that observed[15] for an oxidized Al surface and can be resolved into three components by least-squares fitting. These have been assigned[15] to the bulk oxide (531.5 eV), OH groups (533.0 eV) and H_2O (~534.5 eV). O bonded to C, as well as O in the interfacial SiO_2, could also contribute to the nominal OH peak. The H_2O peak is very weak and barely visible in the spectrum shown in Fig. S3c. A weak satellite, of uncertain origin, is also observed at 537.6 eV. Its separation of ~6 eV from the main peak suggests a possible loss feature due to inter-band excitation. The Al_2O_3 thickness was found to be 8.5 nm with a stoichiometry of n_O/n_{Al} = 1.69, where the O 1s intensity includes both the oxide and OH peaks in Fig. S4. An n_O/n_{Al} somewhat in excess of the ideal value of 1.5 is typical for Al_2O_3 films deposited by RF magnetron sputtering[23]. The C coverage is estimated to be 4.3×10^{15} atoms/cm^2, which is higher than the value of 2.3×10^{15} atoms/cm^2 found in Sec. S5 for SiO_2. Here again (cf. Sec. S5), the molecular coverage (organic molecules/cm^2) is substantially less than the average C coverage (atoms/cm^2)

S7. Surface analysis of hydroxylated Al_2O_3 using XPS

This section presents an analysis of the hydroxylated-Al_2O_3 XPS data (Figs. S3 and S5). The Al, C and O BEs were shifted by -1.7 eV so as to bring the main C 1s peak to 285.5 eV in agreement with the SiO_2 data (Sec. S5). The discussion of this shift given in Sec. S6 also applies here. Here again (cf. Sec. S6) there was no apparent charging shift of the Si 2p spectrum.

The Al 2p is at 74.5 eV, as for the sputter-deposited oxide, and again shows no evidence of sub-oxide structure. The Si 2p data show ~1 nm of Si oxide at the Si/Al_2O_3 interface. The SiO_2 peak is not as well defined as in Fig. S1a, indicating the presence of structure[1] due to SiO_x ($x<2$) in the region between the Si and SiO_2 peaks. For the O 1s peak, the approximately equal intensities of the OH and oxide peaks, together with the stronger H_2O peak, indicate a high degree of hydroxylation. This is typical of O 1s spectra observed[24,25] for AlO(OH) in the so-called "pseudoboehmite" or "poorly-crystalline boehmite" form, which is produced when Al metal or Al_2O_3 is immersed in boiling H_2O as was done here (see Sec. 3.3 of the main text). The film thickness was found to be 5.5 nm with a stoichiometry of $n_O/n_{Al} = 2.3$. The latter result is also typical of XPS data[24,25] for pseudoboehmite AlO(OH) thin films. The C coverage was found to be 3.0×10^{15} atoms/cm^2, which is close to the value found for SiO_2 in Sec. S5 above.

S8. Characterization of *a*-SiO_2 and *a*-Al_2O_3 films using IR transmission

Figures S6 and S7 show normal-incidence IR transmission data for typical thin-film samples. The SiO_2 transverse optic (TO) mode in the 1000-1100 cm^{-1} range is characteristic[26] of a thin oxide film on Si. This mode arises from the asymmetric stretching vibration of the SiO_4 tetrahedra. The corresponding symmetric-stretching TO mode gives rise to a weak absorption at 800 cm^{-1}, part of which is visible in Fig. S6a. For the UV/O_3 oxide, the peak energy (1047 cm^{-1}) is typical for a ~2-nm-thick film on Si (100) and is lower than that for the thicker thermal oxide, seen here at 1073 cm^{-1}. Several explanations have been proposed[27] for the blue-shift with increasing thickness, an analysis of which is beyond the scope of the present work.

For Al_2O_3, transmission spectra computed from the bulk optical constants are shown in Fig. S7 together with data for the present samples. The optical constants were computed from the

Lorentz oscillator parameters reported for α-Al_2O_3 (ref 28) and for γ- and amorphous Al_2O_3 (ref 29). The various forms of Al_2O_3 exhibit very different IR spectra. The calculated spectrum for amorphous material agrees very well with the normal-incidence transmission spectrum[30] of a 0.51 μm-thick *a*-Al_2O_3 film sputter-deposited on a Si wafer. In the present work, *a*-Al_2O_3 was formed on a Ge substrate in order to facilitate the recording of transmission spectra down to 400 cm^{-1}. One spectrum in Fig. S7b was obtained for a sputter-deposited film, and the other was recorded for a film produced by exposure of a 4 nm-thick Al film to UV/O_3. In the later case XPS shows a small amount of metallic Al at the Al_2O_3/Si interface, which does not interfere with the Al_2O_3 spectrum. The conditions for film growth on Ge were identical to those used in fabricating the ATR samples, and the spectra are dominated by a broad band centered at ~680-700 cm^{-1}, which is characteristic of amorphous Al_2O_3. Additional upward-pointing features at about 550 and 840 cm^{-1} are due to amorphous GeO_2 (ref 31), which is present on the air-exposed Ge reference sample but not on the Al_2O_3-coated substrates.

Figure S8 shows IR transmission data for an hydroxylated *a*-Al_2O_3 thin film prepared as described in Sec. 3.3 of the main text. The spectrum is relatively weak in comparison to those for untreated Al_2O_3 (Fig. S7), and only the ν(O-H) bands are clearly discernible, together with structure near 2900 cm^{-1} due to ν(C-H) of organic contaminants and another peak of uncertain origin near 2500 cm^{-1}. The ν(O-H) modes at about 3100 and 3400 cm^{-1} are in good agreement with bands observed[32] at about 3090 and 3400 cm^{-1} for poorly-crystalline (or pseudo) boehmite.

TABLE S1: Parameters Used in Surface Analyses[a]

Parameter	Si	*a*-SiO_2[b]	*a*-Al_2O_3 (AlO(OH))
Density (gm/cm^3)[c]	2.33	2.27	3.20 (3.03)
Molecular Weight (gm)	28.08	60.08	101.96 (59.98)
Si 2p EAL (Å) ($\beta = 1.01$)[d]	31.77	35.72	28.05 (29.92)
O 1s EAL (Å) ($\beta = 2.00$)	N/A	26.01	20.28 (21.68)
Al 2p EAL (Å) ($\beta = 0.93$)	N/A	36.29	28.51 (30.41)
Si 2p Photoionization Cross-section[e]		0.817	
O 1s Photoionization Cross-section		2.93	
Al 2p Photoionization Cross-section[e]		0.537	
C 1s Photoionization Cross-section		1.000	
F 1s Photoionization Cross-section		4.43	
Number of Valence Electrons[f]	N/A	16	24 (16)
Band Gap (eV)[f,g]	N/A	8.9	5.1 (5.6)

(a) "N/A" means "not applicable". All EALs apply to Al Kα excitation. Photoionization cross-sections are relative to that of the C 1s level.

(b) The quantities listed are those for the UV/O_3 oxide film. Very small differences (~1%) are found between EALs for 2 nm-thick UV/O_3 and 8 nm-thick thermal oxide films, as discussed in the Sec. S1.

(c) Si density from ref 9; *a*-SiO_2 density from ref 8; *a*-Al_2O_3 density from ref 11. It should be noted that the oxide values apply to amorphous, not crystalline, materials. AlO(OH) density from ref 14 for the mineral boehmite.

(d) The asymmetry parameters (β) are from ref 6. The oxide EALs are for 2 nm of UV/O_3 SiO_2, 8 nm of *a*-Al_2O_3 and 5 nm of AlO(OH).

(e) The values given are sums of $2p_{1/2}$ and $2p_{3/2}$ contributions

(f) These terms are used only in the calculation of EALs. The quantities for elemental Si are contained in the EAL database[4] and need not be supplied by the user.

(g) SiO_2 band gap from ref 7; *a*-Al_2O_3 band gap from ref 13; AlO(OH) band gap from ref 15 (see comment near end of Sec. S2).

References for Supporting Information

(1) Himpsel, F. J.; McFeely, F. R.; Taleb-Ibrahimi, A.; Yarmoff, J. A.; Hollinger, G. *Phys. Rev. B* **1988**, *38*, 6084.

(2) Briggs, D.; Seah, M. P. *Practical Surface Analysis*; Wiley: Chichester, UK, 1983.

(3) Powell, C. J.; Jablonski, A. *Surf. Interface Anal.* **2002**, *33*, 211.

(4) Powell, C. J.; Jablonski, A. *NIST Electron Effective-Attenuation-Length Database, Vers. 1.1 (SRD-82)*; U.S. Department of Commerce, National Institute of Standards and Technology; Gaithersburg, MD, 2003. For further information see http://www.nist.gov/srd/nist82.htm .

(5) For a lucid discussion of the terminology and correct usage of the NIST SRD-82 database see Petrovykh, D. Y.; Kimura-Suda, H.; Tarlov, M. J.; Whitman, L. J. *Langmuir* **2004**, *20*, 429.

(6) Reilman, R. F.; Msezane, A.; Manson, S. T. *J. Electron Spectrosc. Relat. Phenom.* **1976**, *8*, 389.

(7) Laughlin, R. B. *Phys. Rev. B* **1980**, *22*, 3021.

(8) Fukano, A.; Oyanagi, H. *J. Appl. Phys.* **2003**, *94*, 3345.

(9) *Handbook of Chemistry and Physics, 57th Edition*; Weast, R. C., Ed.; CRC Press: Cleveland, OH, 1977.

(10) Hricovini, K.; Günther, R.; Thiry, P.; Taleb-Ibrahimi, A.; Indlekofer, G.; Bonnet, J. E.; Dumans, P.; Petroff, Y.; Blase, X.; Zhu, X.; Louie, S. G.; Chabal, Y. J.; Thiry, P. A. *Phys. Rev. Lett.* **1993**, *70*, 1992.

(11) Momida, H.; Hamada, T.; Takagi, Y.; Yamamoto,T.; Uda, T.; Ohno, T. *Phys. Rev. B* **2006**, *73*, 054108.

(12) Scofield, J. H. *J. Electron Spectrosc. Relat. Phenom.* **1976**, *8*, 129.

(13) Goodman, A. W. *J. Appl. Phys.* **1970**, *41*, 2176.

(14) http://www.webmineral.com/

(15) Yu, Z. Q.; Wang, C. X.; Xiao, T. G.; Cun, L. *J. Lumin.* **2004**, *106*, 153.

(16) Tielens, F.; Gervais, C.; Lambert, J. F.; Mauri, F.; Costa, D. *Chem. Mater.* **2008**, *20*, 3336.

(17) Powell, C. J. *Appl. Surf. Sci.* **1995**, *89*, 141.

(18) Wagner, C. D.; Naumkin, A. V.; Kraut-Vass, A.; Allison, J. W.; Powell, C. J.; Rumble, J. R., Jr. *NIST X-ray Photoelectron Spectroscopy Database, Vers. 3.5 (SRD-20)*; U.S. Department of Commerce, National Institute of Standards and Technology; Gaithersburg, MD, 2003. For further information see http://srdata.nist.gov/xps/ .

(19) McCafferty, E.; Wightman, J. P. *Surf. Interface Anal.* **1998**, *26*, 549.

(20) Bermudez, V. M.; Berry, A. D.; Kim, H.; Piqué, A. *Langmuir* **2006**, *22*, 11113.

(21) Mullins, W. M.; Averbach, B. L. *Surf. Sci.* **1988**, *206*, 52.

(22) Cordier, F.; Olivier, E. *Surf. Interface Anal.* **1995**, *23*, 601.

(23) Voigt, M.; Bergmaier, A.; Dollinger, G.; Sokolowski, M. *J. Vac. Sci. Technol. A* **2009**, *27*, 234.

(24) Kloprogge, J. T.; Duong, L. V.; Wood, B. J.; Frost, R. L. *J. Colloid Interface Sci.* **2006**, *296*, 572.

(25) Alexander, M. R.; Thompson, G. E.; Beamson, G. *Surf. Interface Anal.* **2000**, *29*, 468.

(26) Queeney, K. T.; Weldon, M. K.; Chang, J. P.; Chabal, Y. J.; Gurevich, A. B.; Sapjeta, J.; Opila, R. L. *J. Appl. Phys.* **2000**, *87*, 1322.

(27) Giustino, F.; Pasquarello, A. *Phys. Rev. Lett.* **2005**, *95*, 187402.

(28) Barker, A. S., Jr. *Phys. Rev.* **1963**, *132*, 1474.

(29) Chu, Y. T.; Bates, J. B.; White, C. W.; Farlow, G. C. *J. Appl. Phys.* **1988**, *64*, 3727.

(30) Brüesch, P.; Kötz, R.; Neff, H.; Pietronero, L. *Phys. Rev. B* **1984**, *29*, 4691.

(31) Galeener, F. L.; Leadbetter, A. J.; Stringfellow, M. W. *Phys. Rev. B* **1983**, *27*, 1052.

(32) Wang, S.-L.; Johnston, C. T.; Bish, D. L.; White, J. L.; Hem, S. L. *J. Colloid Interface Sci.* **2003**, *260*, 26.

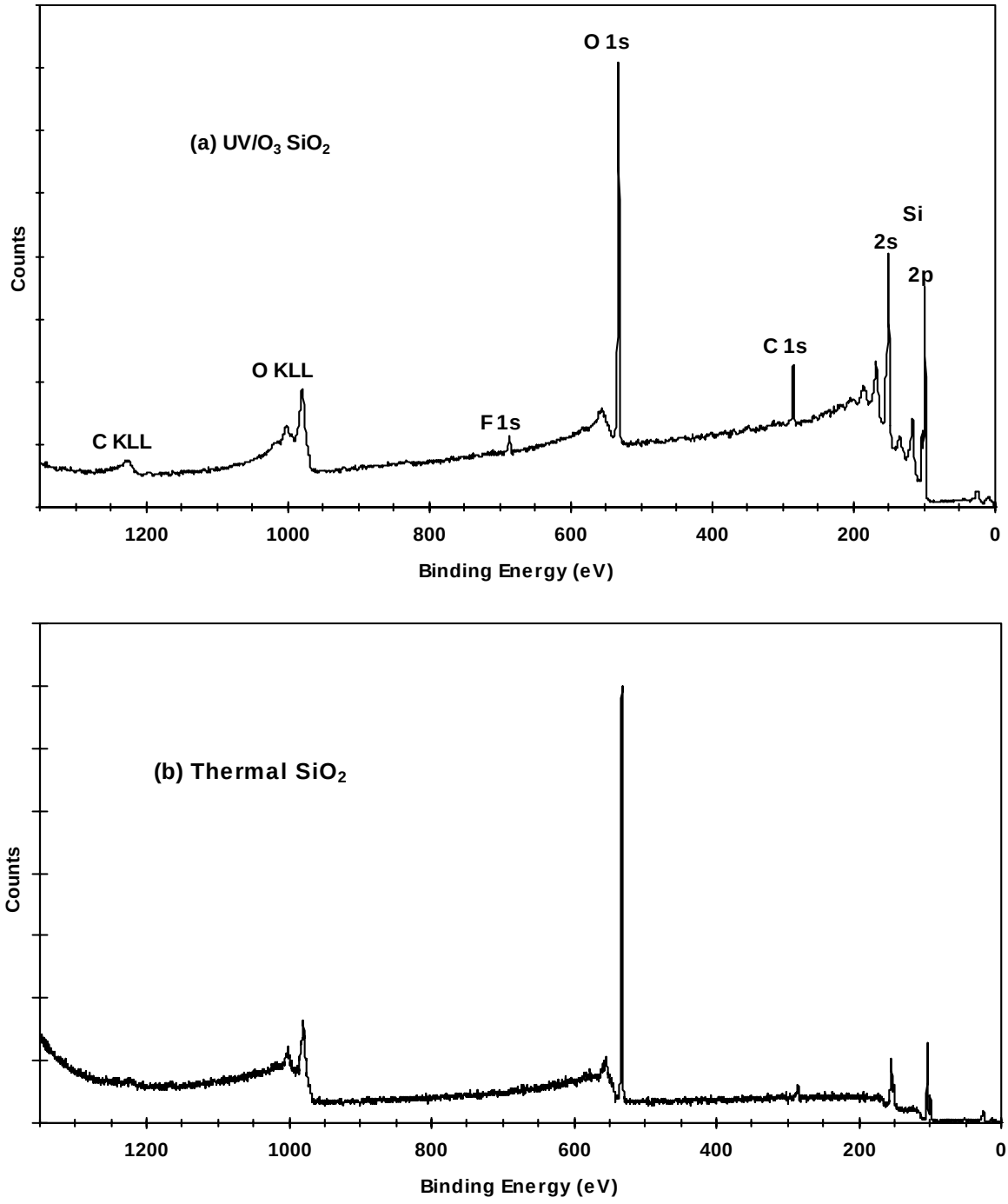

Fig. S1 Typical XPS survey spectra for (a) UV/O_3 *a*-SiO_2 and (b) thermal SiO_2 samples. The KLL features are x-ray-excited Auger emissions.

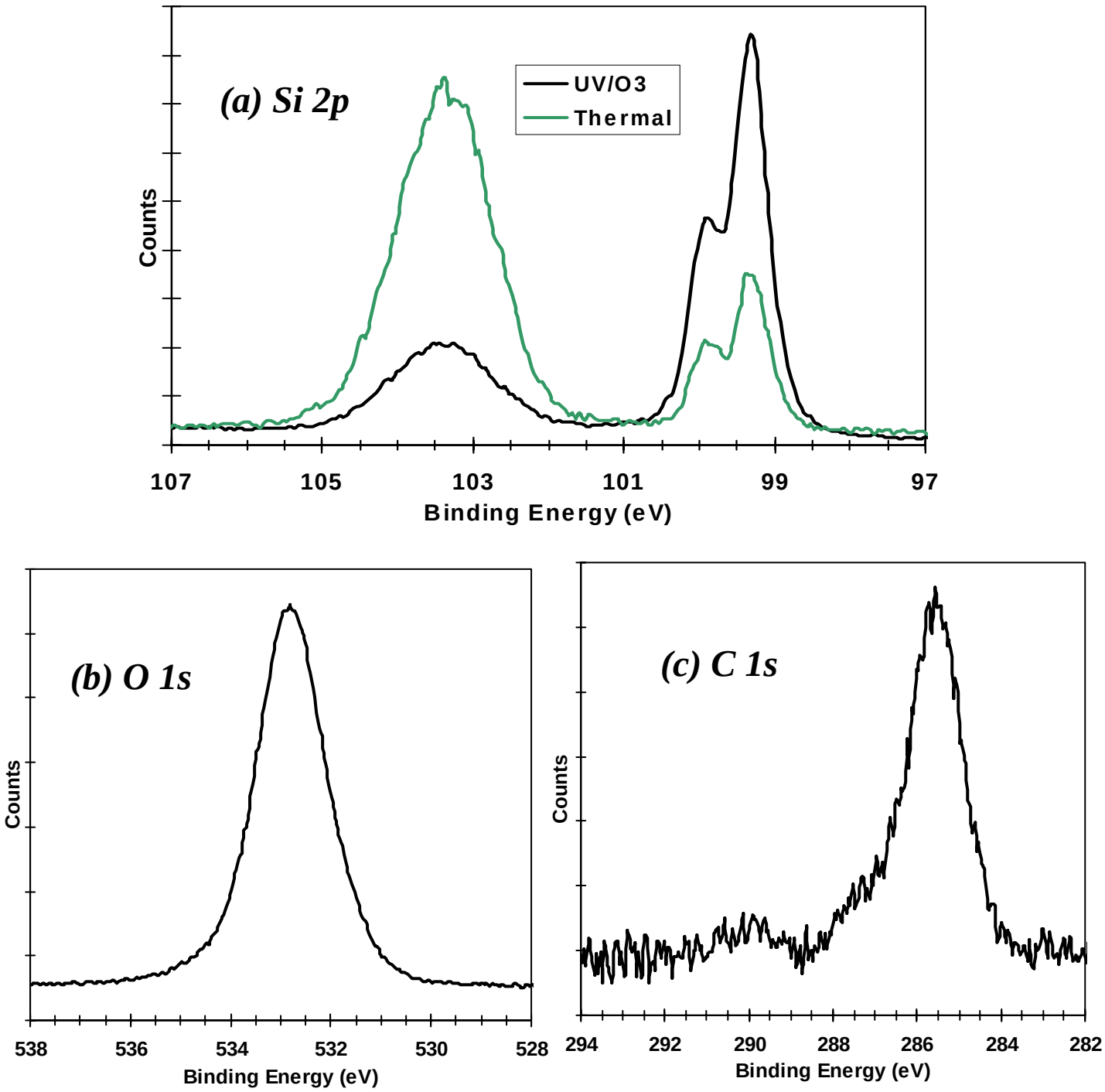

Fig. S2 Typical Al Kα XPS data for SiO_2. All spectra are for a 2.1-nm-thick UV/O_3 sample except for the Si 2p shown in green, which is for a 8.1-nm-thick thermal oxide. The resolution is 0.60 eV. The relative intensities of different spectra are not to scale.

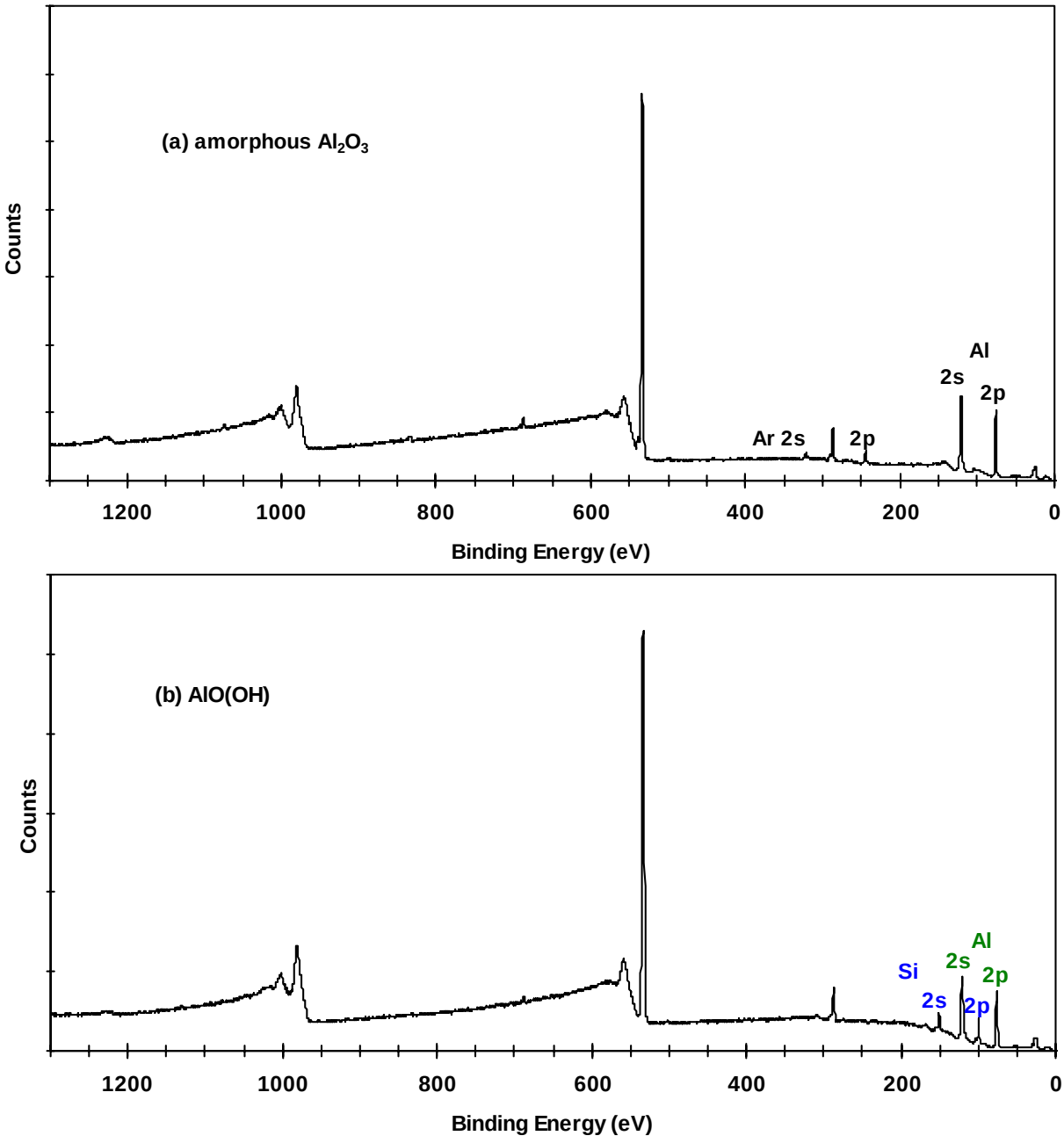

Fig. S3 Similar to Fig. S1 but for (a) sputter-deposited *a*-Al_2O_3 and (b) AlO(OH) formed by immersion of an *a*-Al_2O_3 film in boiling H_2O. See Fig. S1 for additional peak labels. In (a) the argon is implanted during the sputter-deposition process.

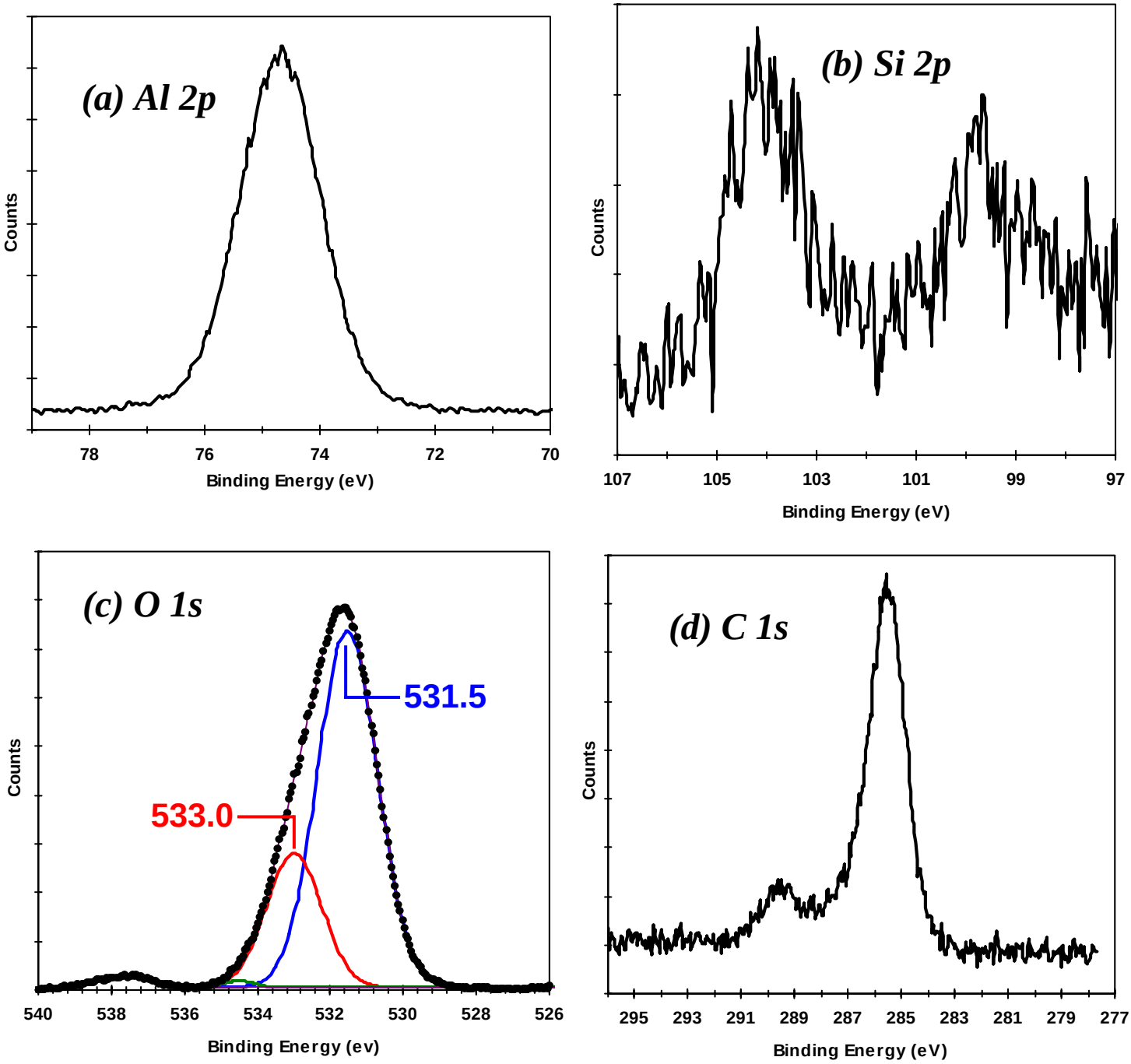

Fig. S4 Similar to Fig. S2 but for 8.5 nm-thick sputter-deposited *a*-Al_2O_3. The O 1s spectrum (points) has been least-squares fitted with a sum of four Gaussian functions and a polynomial background. The fitted background has been subtracted from the data for display. A very weak and barely-visible peak at ~534.5 eV, shown in green, is assigned to molecular H_2O (cf. Sec. S6).

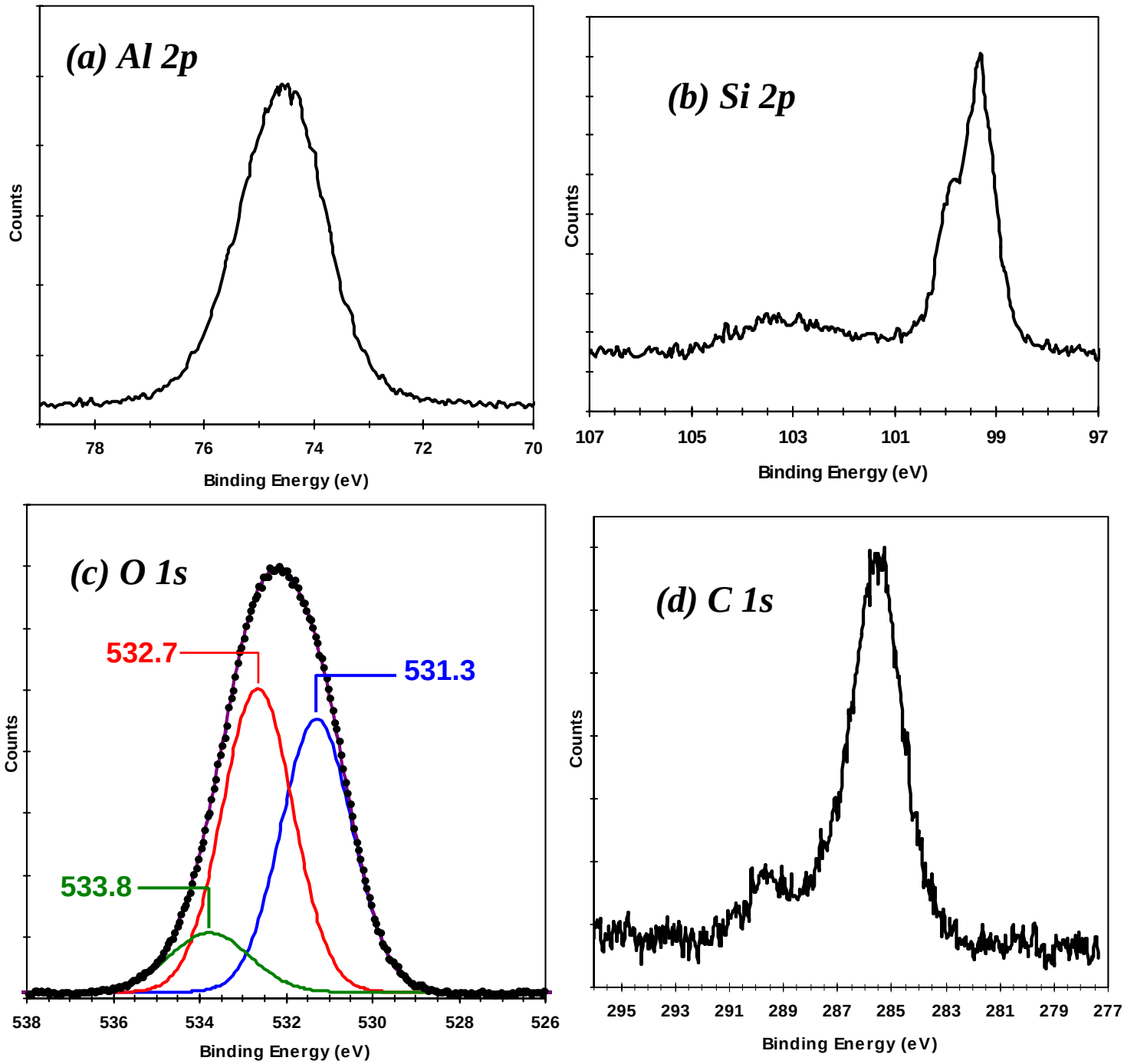

Fig. S5 Similar to Fig. S4 but for a 5.5 nm-thick AlO(OH) film. The resolution is 0.60 eV. The O 1s spectrum shows the result of least-squares fitting the raw data (points) with three Gaussian functions and a polynomial background. The fitted background function has been subtracted for the purpose of display. The line through the points shows the sum of the three peaks.

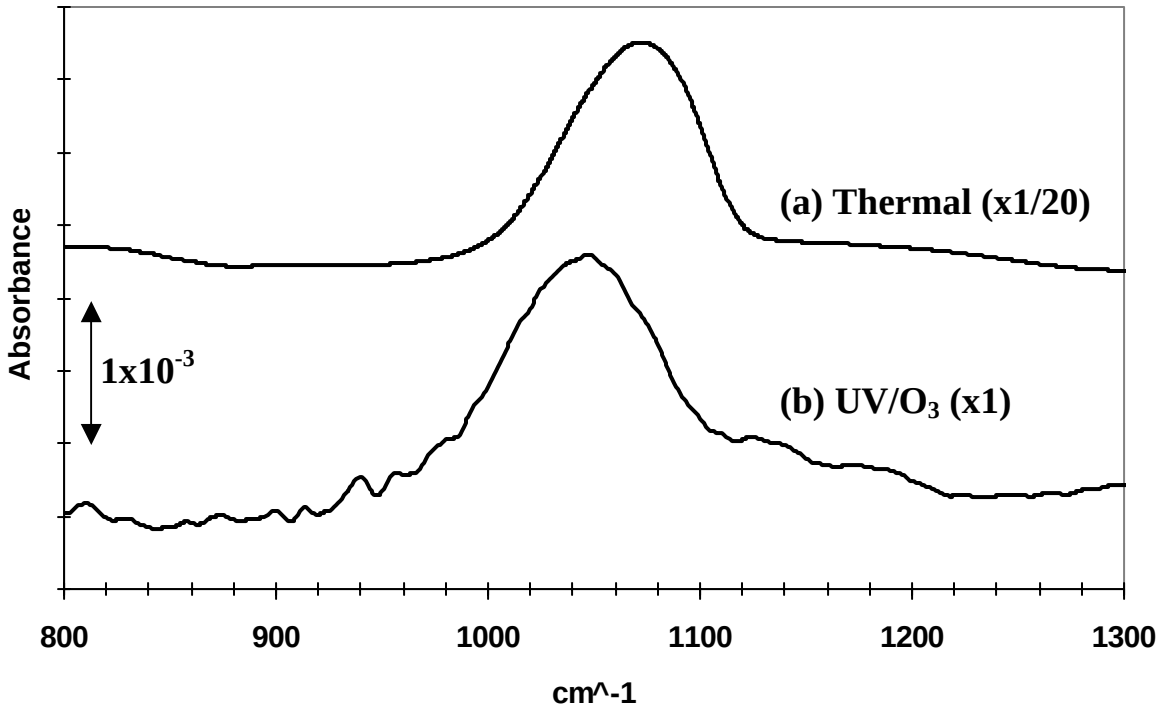

Fig. S6 Normal-incidence transmission spectrum showing the TO phonon absorption for (a) a 8.1-nm-thick thermal oxide and (b) a 2.1-nm-thick UV/O_3 oxide film grown on both sides of a Si ATR prism of unknown crystallographic orientation. The peak is at 1073 cm^{-1} for (a) and at 1047 cm^{-1} for (b). The absorbance scale applies to trace (b). The absorbance scale for trace (a) has been divided by a factor of 20, and the spectra have been displaced vertically for clarity.

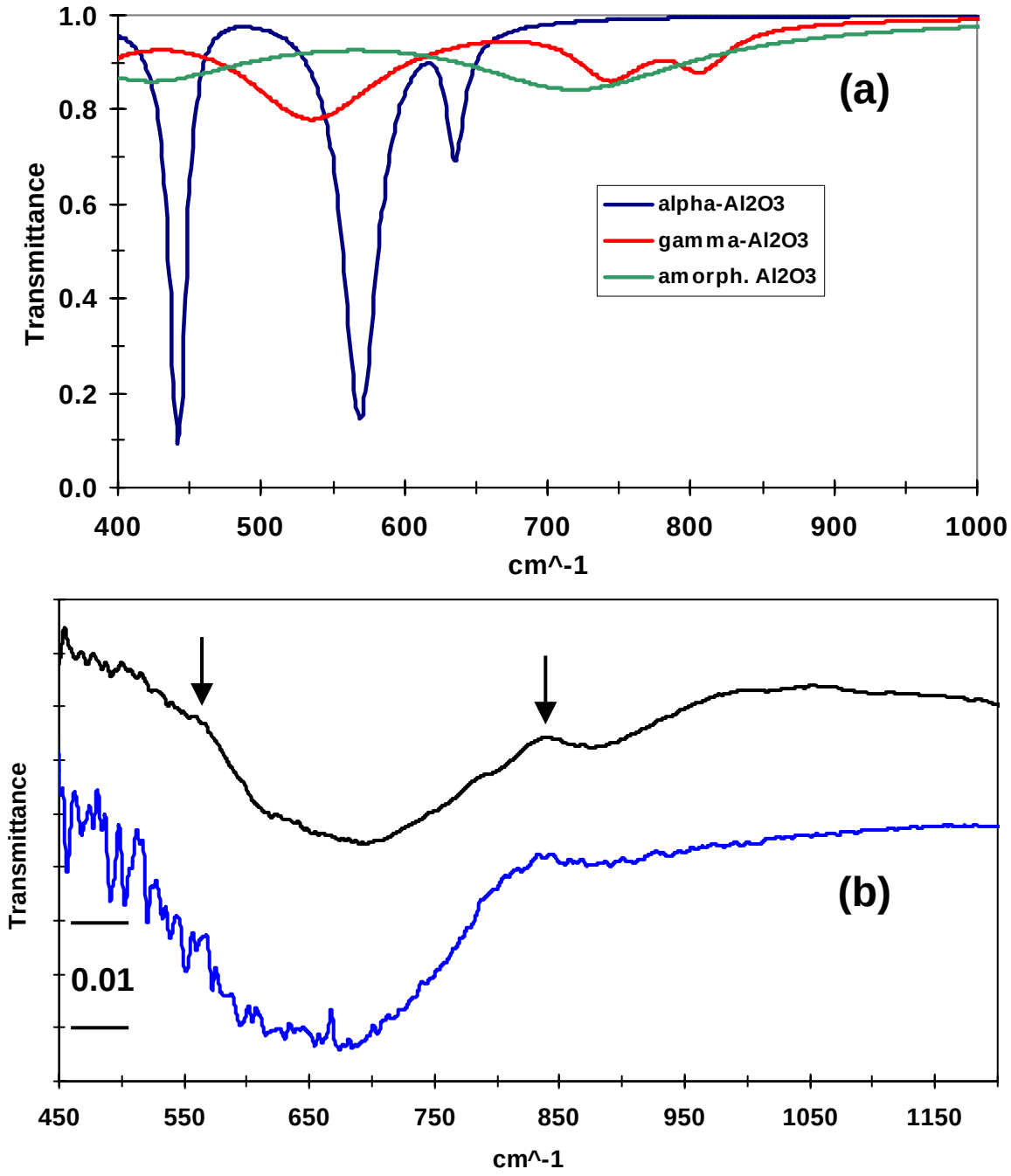

Fig. S7 (a) Normal-incidence transmission spectra for free-standing films of α, γ- and amorphous Al_2O_3 computed using Lorentz oscillator parameters (refs 28,29). For α-Al_2O_3 only the E_u modes are shown, which apply for light propagating along the (0001) crystal axis. The film thicknesses are arbitrarily set at 60 nm. The spectra show only single-phonon TO excitations. (b) Transmission spectra for *a*-Al_2O_3 films grown on a Ge substrate, referenced to that of bare Ge. Features marked with arrows are due to GeO_2 on the reference sample, which is absent on the Al_2O_3-coated surface. Note the different energy and intensity scales for the two figures. The black trace is for a UV/O_3-oxidized Al film, and the blue trace is for sputter-deposited Al_2O_3.

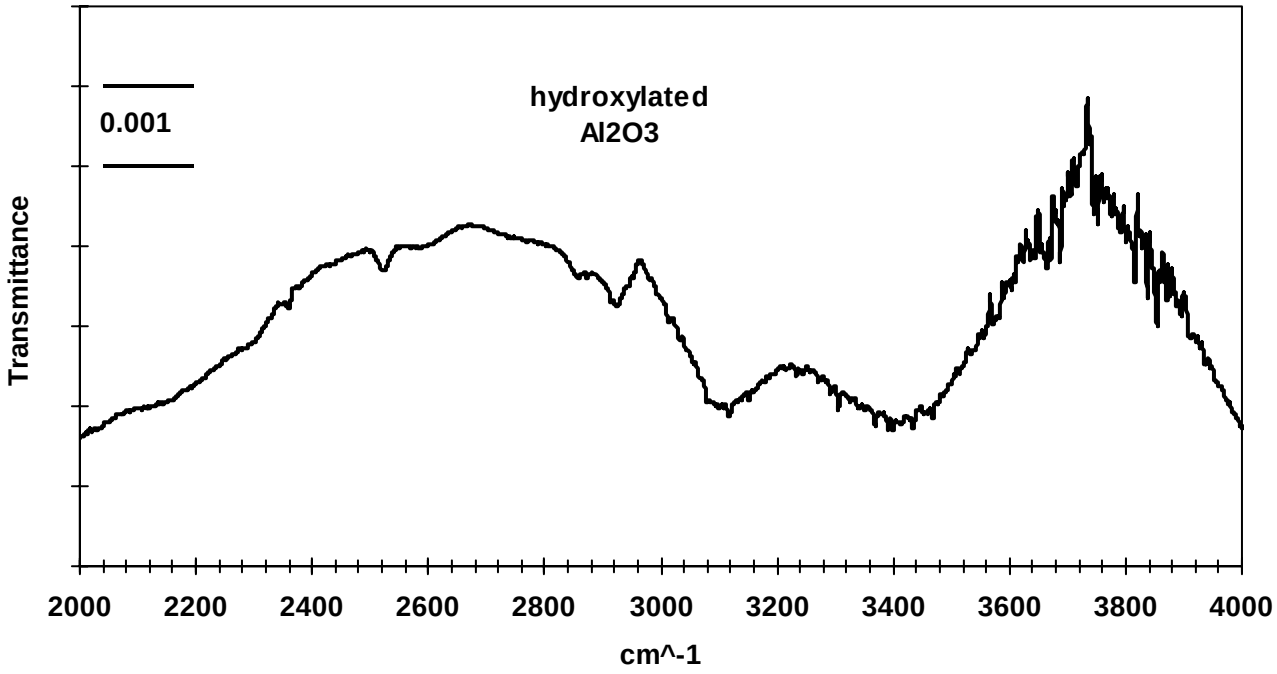

Fig. S8 Normal-incidence transmission spectrum of an *a*-Al_2O_3 thin film on Si hydroxylated by immersion in boiling H_2O. The reference spectrum was obtained for a bare Si substrate. The major features are the ν(O-H) bands at about 3100 and 3400 cm^{-1}.